High-Throughput In-Device Screening of Printable Lead-Free Halide Perovskite Memristors via Machine Learning-Driven Optimization

Emha Bayu Miftahullatif[*1] **Can Cuhadar**[1] **Rohit Attri**[1] **Shreyas Dinesh Pethe**[1] **Nripan Mathews**[12] **Kedar Hippalgaonkar**[1]
[1]*[School of Materials Science and Engineering (MSE), Nanyang Technological University, 50 Nanyang Avenue, Singapore 639798]*
[2]*[Energy Research Institute at Nanyang Technological University (ERI@N), Research Techno Plaza, X-Frontier Block Level 5, 50 Nanyang Drive, Singapore 637553]*

Correspondence to: [Kedar Hippalgaonkar] kedar@ntu.edu.sg

1. Introduction

The growing demand for efficient computing architectures has highlighted the limitations of von Neumann systems, where memory-processor separation creates critical performance bottlenecks. Memristors, which integrate memory and processing functionalities, offer a compelling pathway toward in-memory and neuromorphic computing. [1] Among candidate materials, halide perovskites stand out for their tunable optoelectronic properties, facile processability, and unique ionic migration characteristics. [2] While lead-based compositions were initially explored, toxicity concerns have shifted focus toward lead-free alternatives. However, the halide perovskite materials reported for memristive applications remain limited, and no comprehensive study has systematically explored this broader material space.

Here, we present a high-throughput experimental workflow integrated with machine learning-driven optimization,[4] enabling systematic performance comparison and accelerating the discovery of optimized candidates for next-generation neuromorphic technologies.

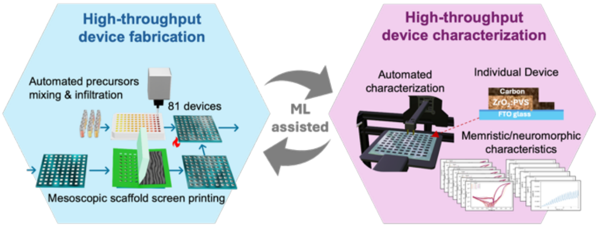

Fig. 1: High-throughput platform combining device fabrication, device characterization, and driven by Machine Learning.

2. Experiment

To systematically explore the halide perovskite material space for memristor applications, we developed a high-throughput platform integrating screen-printed device fabrication, automated precursor mixing, comprehensive electrical characterization, and machine learning-driven optimization (Fig. 1).

2.1 Device Fabrication and Material Screening

Devices were fabricated by screen-printing 81 arrays of scaffold cells on fluorine-doped tin oxide (FTO) glass substrates, each consisting of a mesoporous ZrO_2 spacer layer and a carbon electrode. Active layers were formed by infiltrating scaffolds with precursor solutions, followed by controlled crystallization. To explore a broad composition space, a liquid handling robot precisely mixed 20 precursor solutions spanning inorganic halides (RbI, RbBr, CsI, CsBr), organic halides (MAI, MABr, FAI, FABr, AVAI, PEAI, GI, BAI), and metal halides (AgI, AgBr, CuI, CuBr, BiI_3, $BiBr_3$, SbI_3, $SbBr_3$). Initial compositions were designed using Latin Hypercube Sampling (LHS) to ensure broad material space coverage, enabling the formation of diverse end-products including 2D/3D perovskites, perovskite-inspired structures (e.g., pnictohalides), and materials with stoichiometric variations.

2.2 Memristor Characterization and Machine Learning workflow

Voltage pulse-driven potentiation and depression tests were performed on each device to evaluate synaptic characteristics. Potentiation gain (*Pot_gain*, reflecting conductance increase magnitude) and potentiation non-linearity (*Pot_gamma*) were selected as primary optimization targets, aiming to maximize and minimize each metric, respectively. Iterative experimental campaigns were conducted using both Bayesian Optimization and LLM-guided strategies to navigate the composition space efficiently.

To represent each precursor formulation as a machine learning-compatible input, we developed a role-aware descriptor engineering pipeline that decomposes each composition into four chemically meaningful site roles: inorganic A-site cations (Rb, Cs), organic A-site cations (MA, FA, AVA, PEA, GA, BA), B-site metals (Cu, Ag, Bi, Sb), and X-site halides (I, Br).

Composition-weighted physicochemical descriptors were computed using pymatgen, matminer, and RDKit. Six machine learning models were trained and evaluated via out-of-fold cross-validation. SHAP analysis was applied to quantify descriptor contributions and inform rational material design.

3. Results

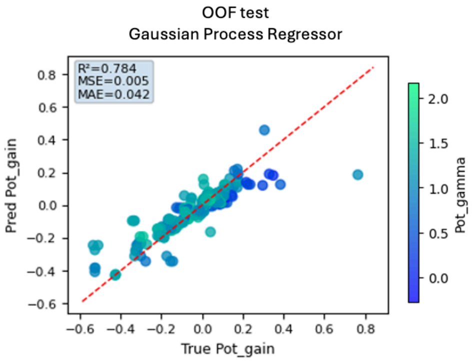

Fig. 2: Out-of-Fold test results of the Gaussian Process Regressor as the best performing model.

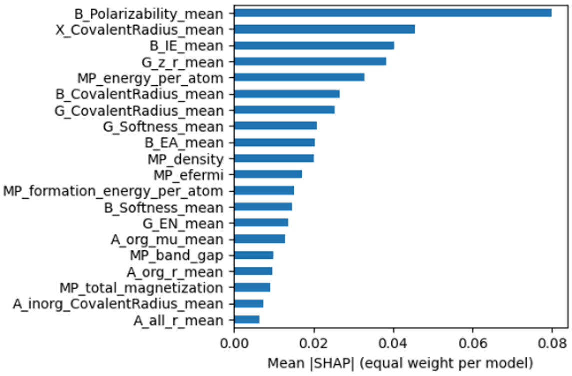

Fig. 3: Mean SHAP value from the top 4 models predicting *Pot_gain*.

Among six trained models, the Gaussian Process Regressor achieved the best predictive performance for *Pot_gain*, with $R^2 = 0.784$, MSE = 0.005, and MAE = 0.042 on out-of-fold validation (Fig. 2). Prediction of *Pot_gamma* remained unsatisfactory, suggesting greater compositional complexity, or measurement setting governing non-linearity, warranting further investigation.

To interpret model predictions and extract compositional design rules SHAP analysis was conducted. Ensemble SHAP analysis across the top four models (Fig. 3) identified B-site polarizability, X-site covalent radius, and B-site ionization energy as the top 3 influential descriptors for *Pot_gain*. Contour analysis across the top five descriptors (Fig. 4) further reveals that compositions with lower B-site polarizability, larger X-site covalent radius, and lower B-site ionization energy are associated with enhanced potentiation gain — providing interpretable design guidelines for targeted material synthesis.

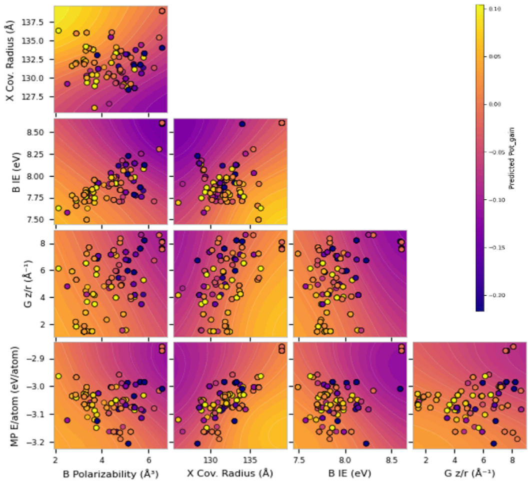

Fig. 4: Contour plot of top 5 important descriptors.

Collectively, these results demonstrate the capability of our high-throughput platform to efficiently navigate a complex halide perovskite composition space, uncovering physically meaningful component–property relationships that can guide the rational discovery of high-performance memristor candidates for neuromorphic and next-generation memory applications.

Acknowledgments

The authors acknowledge the funding support from National Research Foundation (NRF), Singapore, under its Competitive Research Program (CRP) (NRF-CRP25-2020-0002).

References

[1] “The memristor revisited,” *Nat Electron*, vol. 1, no. 5, pp. 261–261, May 2018, doi: 10.1038/s41928-018-0083-3.

[2] K. Sakhatskyi *et al.*, “Assessing the Drawbacks and Benefits of Ion Migration in Lead Halide Perovskites,” *ACS Energy Lett.*, vol. 7, no. 10, pp. 3401–3414, Oct. 2022, doi: 10.1021/acsenergylett.2c01663.

[3] B. W. Zhang *et al.*, “Lead-Free Perovskites and Metal Halides for Resistive Switching Memory and Artificial Synapse,” *Small Structures*, vol. 5, no. 6, Jun. 2024, doi: 10.1002/sstr.202300524.

[4] E. B. Miftahullatif *et al.*, "Machine-Learning-Driven in-Device Optimization of All-Printed Perovskite Solar Cells," *ACS Energy Lett.*, vol. 10, no. 8, pp. 3952-3961, Aug. 2025, doi: 10.1021/acsenergylett.5c01475.